



**HAL**  
open science

## 6-Chloro-3-nitro-8-(phenylthio)-2-[(phenylthio)methyl]imidazo[1,2-a]pyridine

Romain Paoli-Lombardo, Nicolas Primas, Sébastien Hutter, Sandra Bourgeade-Delmas, Clotilde Boudot, Caroline Castera-Ducros, Inès Jacquet, Bertrand Courtioux, Nadine Azas, Pascal Rathelot, et al.

► **To cite this version:**

Romain Paoli-Lombardo, Nicolas Primas, Sébastien Hutter, Sandra Bourgeade-Delmas, Clotilde Boudot, et al.. 6-Chloro-3-nitro-8-(phenylthio)-2-[(phenylthio)methyl]imidazo[1,2-a]pyridine. Molbank, 2023, 2023 (2), pp.M1613. 10.3390/M1613. hal-04275810

**HAL Id: hal-04275810**

**<https://hal.science/hal-04275810>**

Submitted on 14 Nov 2023

**HAL** is a multi-disciplinary open access archive for the deposit and dissemination of scientific research documents, whether they are published or not. The documents may come from teaching and research institutions in France or abroad, or from public or private research centers.





L'archive ouverte pluridisciplinaire **HAL**, est destinée au dépôt et à la diffusion de documents scientifiques de niveau recherche, publiés ou non, émanant des établissements d'enseignement et de recherche français ou étrangers, des laboratoires publics ou privés.



Distributed under a Creative Commons Attribution 4.0 International License

Short Note

# 6-Chloro-3-nitro-8-(phenylthio)-2-[(phenylthio)methyl]imidazo[1,2-*a*]pyridine

Romain Paoli-Lombardo <sup>1</sup>, Nicolas Primas <sup>1,2,\*</sup>, Sébastien Hutter <sup>3</sup>, Sandra Bourgeade-Delmas <sup>4</sup>, Clotilde Boudot <sup>5</sup>, Caroline Castera-Ducros <sup>1,2</sup>, Inès Jacquet <sup>1</sup>, Bertrand Courtioux <sup>5</sup>, Nadine Azas <sup>3</sup>, Pascal Rathelot <sup>1,2</sup> and Patrice Vanelle <sup>1,2,\*</sup>

<sup>1</sup> CNRS, ICR UMR 7273, Team Pharmaco-Chimie Radicalaire, Faculté de Pharmacie, Aix Marseille University, 27 Boulevard Jean Moulin, CS30064, CEDEX 05, 13385 Marseille, France; romain.paoli-romain.paoli-lombardo@etu.univ-amu.fr (R.P.-L.); caroline.ducros@univ-amu.fr (C.C.-D.); ines.jacquet@etu.univ-amu.fr (I.J.); pascal.rathelot@univ-amu.fr (P.R.)

<sup>2</sup> AP-HM, Service Central de la Qualité et de l'Information Pharmaceutiques, Hôpital de la Conception, 13005 Marseille, France

<sup>3</sup> IHU Méditerranée Infection, UMR VITROME-Tropical Eukaryotic Pathogens, Aix Marseille University, 19–21 Boulevard Jean Moulin, 13005 Marseille, France; sebastien.hutter@univ-amu.fr (S.H.); nadine.azas@univ-amu.fr (N.A.)

<sup>4</sup> UMR 152 PHARMA-DEV, University of Toulouse, IRD, 31062 Toulouse, France; sandra.bourgeade-delmas@ird.fr

<sup>5</sup> UMR Inserm 1094, Neuroépidémiologie Tropicale, Faculté de Pharmacie, University of Limoges, 2 Rue Du Dr Marcland, 87025 Limoges, France; bertrand.courtioux@unilim.fr (B.C.)

\* Correspondence: nicolas.primas@univ-amu.fr (N.P.); patrice.vanelle@univ-amu.fr (P.V.)

**Abstract:** As part of our ongoing antikinoplastid structure–activity relationship study focused on positions 2 and 8 of the 3-nitroimidazo[1,2-*a*]pyridine scaffold, we were able to introduce a phenylthioether moiety at both position 2 and position 8 in one step. Using a previously reported synthetic route developed in our laboratory, we obtained 6-chloro-3-nitro-8-(phenylthio)-2-[(phenylthio)methyl]imidazo[1,2-*a*]pyridine in 74% yield. The in vitro cell viability of this compound was assessed on the HepG2 cell line, and its in vitro activity was evaluated against the promastigote form of *L. donovani*, the axenic amastigote form of *L. infantum* and the trypomastigote blood stream form of *T. b. brucei*. It showed low solubility in HepG2 culture medium ( $CC_{50} > 7.8 \mu\text{M}$ ), associated with weak activity against both the promastigote form of *L. donovani* ( $EC_{50} = 8.8 \mu\text{M}$ ), the axenic amastigote form of *L. infantum* ( $EC_{50} = 9.7 \mu\text{M}$ ) and the trypomastigote blood stream form of *T. b. brucei* ( $EC_{50} = 12.8 \mu\text{M}$ ).

**Keywords:** imidazo [1,2-*a*] pyridine; nitroaromatic; structure–activity relationship; *Leishmania* spp.; *Trypanosoma brucei*



**Citation:** Paoli-Lombardo, R.; Primas, N.; Hutter, S.; Bourgeade-Delmas, S.; Boudot, C.; Castera-Ducros, C.; Jacquet, I.; Courtioux, B.; Azas, N.; Rathelot, P.; et al. 6-Chloro-3-nitro-8-(phenylthio)-2-[(phenylthio)methyl]imidazo[1,2-*a*]pyridine. *Molbank* **2023**, *2023*, M1613. <https://doi.org/10.3390/M1613>

Academic Editor: Nicholas E. Leadbeater

Received: 8 March 2023

Revised: 21 March 2023

Accepted: 27 March 2023

Published: 30 March 2023



**Copyright:** © 2023 by the authors. Licensee MDPI, Basel, Switzerland. This article is an open access article distributed under the terms and conditions of the Creative Commons Attribution (CC BY) license (<https://creativecommons.org/licenses/by/4.0/>).

## 1. Introduction

In humans, kinetoplastid diseases are caused by flagellated protozoa of the genus *Leishmania* and *Trypanosoma* [1]. Leishmaniases (*Leishmania* spp.) and sleeping sickness (*Trypanosoma brucei*) are defined by the World Health Organization (WHO) as neglected tropical diseases (NTDs), mainly present in developing countries [2]. Threatening more than one billion people worldwide, these two diseases are responsible for nearly 50,000 deaths per year [3,4].

Among the twenty species of *Leishmania* responsible for infection in people, two are responsible for life-threatening visceral leishmaniasis (VL): *L. donovani* in Asia and Africa, and *L. infantum* in the Mediterranean Basin and Latin America [5]. Between 50,000 and 90,000 new cases and more than 30,000 deaths due to VL are reported annually [6]. For sleeping sickness, about 60 million people in 36 sub-Saharan African countries are considered to be at risk of contracting it [7]. Since 2019, less than 1000 cases are recorded

by the WHO annually, but this number is probably underestimated because of the under-diagnosis of the disease [8]. In the absence of a vaccine [9], VL and sleeping sickness are treated with a small spectrum of very few efficient, safe and affordable drugs [10].

As part of our research program to develop new potential antikinetooplastid derivatives in the 3-nitroimidazo[1,2-*a*]pyridine series, our team previously described a hit molecule (Hit A), bearing a phenylsulfonylmethyl substituent at position 2; a chlorine atom at position 6 and a 4-chlorophenylthioether moiety at position 8 (Table 1) [11]. Its influence on cell viability (cytotoxic concentration 50% = CC<sub>50</sub>) was assessed on the human hepatocyte HepG2 cell line, showing low cytotoxicity. In vitro activities (measured by the effective concentration 50% = EC<sub>50</sub>) were evaluated against both the promastigote form of *L. donovani*, the axenic amastigote form of *L. infantum* and the trypomastigote bloodstream form (BSF) of *T. b. brucei*. Hit A displayed micromolar activities on all these forms.

**Table 1.** Structures and biological profiles of previously identified Hit A and Molecule B.

	Hit A	Molecule B
EC <sub>50</sub> <i>L. donovani</i> promastigotes (μM)	1.0 ± 0.3	7.4 ± 0.4
EC <sub>50</sub> <i>L. infantum</i> axenic amastigotes (μM)	1.7 ± 0.3	-
EC <sub>50</sub> <i>T. b. brucei</i> BSF (μM)	0.95 ± 0.05	>50
CC <sub>50</sub> HepG2 (μM)	>100	>15.6

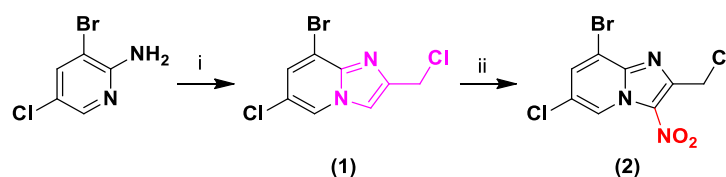
After identifying this hit compound, a phenylthiomethyl analogue (Molecule B) was obtained and evaluated in vitro (Table 1) [12]. Replacement of the sulfone with a sulfur atom resulted in decreased solubility in HepG2 culture medium and decreased antileishmanial activity, as well as a loss of antitrypanosomal activity.

Throughout our structure–activity relationship study focused on positions 2 and 8 of the 3-nitroimidazo[1,2-*a*]pyridine scaffold; we were able to introduce a phenylthioether moiety at both position 2 and position 8. This allowed us to replace the sulfone at position 2 with a sulfur atom and remove the chlorine atom at the para position of the phenyl ring at position 8, using a single reaction.

## 2. Results and Discussion

### 2.1. Synthesis

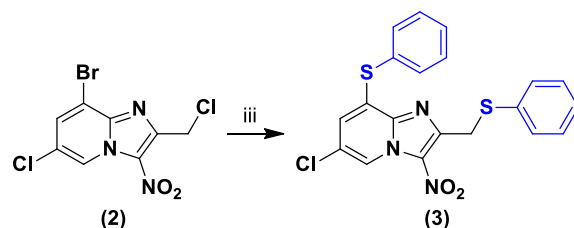
Using a previously described synthetic route developed in our laboratory [13], 3-bromo-5-chloropyridin-2-amine was cyclized into the corresponding 2-chloromethylimidazo[1,2-*a*]pyridine intermediate 1 by reaction with 1,3-dichloroacetone in refluxing ethanol, followed by a selective nitration reaction at the position 3, giving 3-nitroimidazo[1,2-*a*]pyridine derivative 2 (Scheme 1).



**Scheme 1.** Synthesis of compounds (1) and (2).

Reagents and conditions: (i) 1,3-Dichloroacetone 1.1 equiv, EtOH, reflux, 96 h, 60%; (ii) HNO<sub>3</sub> 65% 6 equiv, H<sub>2</sub>SO<sub>4</sub>, 0 °C → RT, 3 h, 60%.

Then, compound 3 was obtained in good yield by substituting both the chlorine atom of the chloromethyl group at position 2 and the bromine atom at position 8 of substrate 2 with sodium thiophenolate formed in situ with NaH in DMSO at room temperature (Scheme 2).



**Scheme 2.** Synthesis of compound (3).

Reagents and conditions: (3) Thiophenol 2 equiv, NaH 60% 2 equiv, DMSO, N<sub>2</sub>, RT, 15 h, 74%.

## 2.2. Biological Results

The cell viability of compound 3 was assessed on the HepG2 cell line, and doxorubicin was used as a positive control. The antileishmanial activity was evaluated in vitro against both the promastigote form of *L. donovani* and the axenic amastigote form of *L. infantum*. The antitrypanosomal activity was determined on the trypomastigote bloodstream form of *T. b. brucei*. Biological profiles were compared to Hit A, Molecule B and reference drugs (amphotericin B, miltefosine, fexinidazole and suramin) (Table 2 and Table S1).

**Table 2.** In vitro evaluation of molecule 3 on the human hepatocyte HepG2 cell line, *L. donovani* promastigotes, *L. infantum* axenic amastigotes and *T. b. brucei* trypomastigotes BSF.

	CC <sub>50</sub> HepG2 ( $\mu$ M)	EC <sub>50</sub> <i>L. Dono.</i> Pro. ( $\mu$ M)	EC <sub>50</sub> <i>L. Inf.</i> Axenic Ama. ( $\mu$ M)	EC <sub>50</sub> <i>T. B. Brucei</i> BSF ( $\mu$ M)
3	>7.8 <sup>a</sup>	8.8 $\pm$ 1.5	9.7 $\pm$ 1.2	12.8 $\pm$ 0.8

<sup>a</sup> The product could not be tested at higher concentrations due to a lack of solubility in the culture medium.

Compared to Hit A, compound 3 showed low solubility in HepG2 culture medium (CC<sub>50</sub> > 7.8  $\mu$ M), associated with decreased activity against both the promastigote form of *L. donovani* (EC<sub>50</sub> = 8.8  $\mu$ M), the axenic amastigote form of *L. infantum* (EC<sub>50</sub> = 9.7  $\mu$ M) and the trypomastigote bloodstream form of *T. b. brucei* (EC<sub>50</sub> = 12.8  $\mu$ M). However, compound 3 displayed similar antileishmanial activity and showed a better antitrypanosomal EC<sub>50</sub> value than Molecule B (EC<sub>50</sub> = 7.4  $\mu$ M and EC<sub>50</sub> > 50  $\mu$ M, respectively).

Thus, the replacement of the sulfone at position 2 with a sulfur atom, leading to Molecule B and compound 3, resulted in both a loss of solubility and a decrease in antileishmanial and antitrypanosomal activity. However, the chlorine atom at the para position of the phenyl ring at position 8 did not appear to be essential to the activity and even led to a slight improvement in antitrypanosomal activity.

## 3. Materials and Methods

### 3.1. Chemistry

#### 3.1.1. General

Melting points were determined on a Köfler melting point apparatus (Wagner & Munz GmbH, München, Germany) and were uncorrected. The infrared (IR) spectrum was measured for pure products on a Bruker VERTEX70 FTIR spectrometer equipped with a Bruker A222 Attenuated Total Reflection (ATR) accessory at the Faculté des Sciences de Saint-Jérôme (Marseille). The crystal used is a diamond. The spectrometer is equipped with a Globar source and a KBr/DLaTGS detector. Each spectrum is recorded with 30 scans and a scanning speed of 10 KHz in the spectral range of 4000–400 cm<sup>-1</sup>. The apodization

function used is Blackman-Harris 3 terms. The spectrometer is continuously purged with dry CO<sub>2</sub>-free air. The spectrum of the ATR accessory without a sample served as a reference. The temperature inside the spectrometer has been kept constant at 25 °C. UV-Vis absorption spectra were recorded at the Faculté des Sciences de Saint-Jérôme (Marseille) with a Jasco V670 instrument equipped with a Peltier cell holder ETCS-761 to maintain the temperature at 20.0 °C. A quartz cell of 1 mm of optical path length was used. Solution of compound 3 with a concentration of 0.16 g.L<sup>-1</sup> was prepared in acetonitrile (HPLC grade). The UV-vis absorption spectra were recorded using the solvent as a reference and are presented without smoothing and further data processing. The measurement range was 200–800 nm with a data interval of 2 nm, a scan speed of 400 nm/min and a UV-vis bandwidth of 2 nm. HRMS spectrum (ESI) was recorded on a SYNAPT G2 HDMS (Waters) at the Faculté des Sciences de Saint-Jérôme (Marseille). NMR spectra were recorded on a Bruker Avance 200 MHz or a Bruker Avance NEO 400 MHz NanoBay spectrometer at the Faculté de Pharmacie of Marseille. (<sup>1</sup>H NMR: reference CDCl<sub>3</sub> δ = 7.26 ppm, reference DMSO-*d*<sub>6</sub> δ = 2.50 ppm and <sup>13</sup>C NMR: reference CDCl<sub>3</sub> δ = 76.9 ppm, reference DMSO-*d*<sub>6</sub> δ = 39.52 ppm). The following adsorbent was used for column chromatography: silica gel 60 (Merck KGaA, Darmstadt, Germany, particle size 0.063–0.200 mm, 70–230 mesh ASTM). TLC was performed on 5 cm x 10 cm aluminum plates coated with silica gel 60F-254 (Merck) in an appropriate eluent. Visualization was performed with ultraviolet light (234 nm). The purity determination of synthesized compounds was checked by LC/MS analyses, which were realized at the Faculté de Pharmacie of Marseille with a Thermo Scientific Accela High-Speed LC System<sup>®</sup> (Waltham, MA, USA) coupled using a single quadrupole mass spectrometer Thermo MSQ Plus<sup>®</sup>. The purity of synthesized compound 3 was > 95%. The RP-HPLC column is a Thermo Hypersil Gold<sup>®</sup> 50 × 2.1 mm (C<sub>18</sub> bounded), with particles of a diameter of 1.9 mm. The volume of the sample injected into the column was 1 μL. Chromatographic analysis, total duration of 8 min, was on the gradient of the following solvents: t = 0 min, methanol/water 50:50; 0 < t < 4 min, linear increase in the proportion of methanol to a methanol/water ratio of 95:5; 4 < t < 6 min, methanol/water 95:5; 6 < t < 7 min, linear decrease in the proportion of methanol to return to a methanol/water ratio of 50:50; 6 < t < 7 min, methanol/water 50:50. The water used was buffered with ammonium acetate 5 mM. The flow rate of the mobile phase was 0.3 mL/min. The retention times (t<sub>R</sub>) of the molecules analyzed were indicated in min. Reagents were purchased from Sigma-Aldrich or Fluorochem and used without further purification. Copies of <sup>1</sup>H NMR, <sup>13</sup>C NMR, IR and UV-Vis spectra are available in the Supplementary Materials.

### 3.1.2. 8-Bromo-6-chloro-2-chloromethylimidazo[1,2-*a*]pyridine (1)

To a solution of 3-bromo-5-chloropyridin-2-amine (5 g, 24.1 mmol, 1 equiv) in ethanol (80 mL), 1,3-dichloroacetone (3.34 g, 26.5 mmol, 1.1 equiv) was added. The reaction mixture was stirred and heated under reflux for 96 h. The solvent was then evaporated in vacuo. Compound 1 was obtained after purification by chromatography on silica gel (dichloromethane) as a yellow solid in 60% yield (4.1 g). mp 161 °C. <sup>1</sup>H NMR (200 MHz, CDCl<sub>3</sub>) δ: 8.13 (d, *J* = 1.6 Hz, 1H), 7.71 (s, 1H), 7.48 (d, *J* = 1.6 Hz, 1H), 4.79 (s, 2H). <sup>13</sup>C NMR (50 MHz, CDCl<sub>3</sub>) δ: 142.0, 137.7, 125.4, 122.4, 120.1, 116.0, 113.0, 39.1. LC/MS ESI + t<sub>R</sub> 1.77 min, (*m/z*) [M + H]<sup>+</sup> 278.80/280.85/282.84. HRMS (+ESI): 280.9064 [M + H]<sup>+</sup>. Calcd for C<sub>8</sub>H<sub>6</sub>BrCl<sub>2</sub>N<sub>2</sub>: 280.9062.

### 3.1.3. 8-Bromo-6-chloro-2-chloromethyl-3-nitroimidazo[1,2-*a*]pyridine (2)

To a solution of 8-bromo-6-chloro-2-chloromethylimidazo[1,2-*a*]pyridine (1) (2 g, 7.2 mmol, 1 equiv) in concentrated sulfuric acid (20 mL) cooled by an ice-water bath, nitric acid 65% (1.9 mL, 43.2 mmol, 6 equiv) was added while keeping the temperature below 0 °C. The reaction mixture was stirred for 3 h at room temperature. Then, the mixture was slowly poured into an ice-water mixture and the desired product precipitated. Compound 2 was obtained after purification by chromatography on silica gel (eluent: dichloromethane)

as a yellow solid in 60% yield (1.4 g). mp 165 °C.  $^1\text{H}$  NMR (200 MHz,  $\text{CDCl}_3$ )  $\delta$ : 9.48 (d,  $J = 1.8$  Hz, 1H), 7.92 (d,  $J = 1.8$  Hz, 1H), 5.08 (s, 2H).  $^{13}\text{C}$  NMR (50 MHz,  $\text{CDCl}_3$ )  $\delta$ : 147.7, 140.9, 134.07, 129.9, 125.2, 124.7, 113.2, 38.2. LC/MS ESI +  $t_{\text{R}}$  2.51 min, ( $m/z$ )  $[\text{M} + \text{H}]^+$  324.00/325.93. HRMS (+ESI): 323.8938  $[\text{M} + \text{H}]^+$ . Calcd for  $\text{C}_8\text{H}_5\text{BrCl}_2\text{N}_3\text{O}_2$ : 323.8937.

### 3.1.4. 6-Chloro-3-nitro-8-(phenylthio)-2-[(phenylthio)methyl]imidazo[1,2-*a*]pyridine (3)

To a sealed 20 mL flask containing sodium hydride (60% dispersion in mineral oil) (0.098 g, 2.46 mmol, 2 equiv) in dimethylsulfoxide (3 mL), thiophenol (253  $\mu\text{L}$ , 2.46 mmol, 2 equiv) was added under  $\text{N}_2$  atmosphere. The reaction mixture was stirred at room temperature for 30 min. Then, a solution of 8-bromo-6-chloro-2-chloromethyl-3-nitroimidazo[1,2-*a*]pyridine (2) (0.4 g, 1.23 mmol, 1 equiv) in dimethylsulfoxide (6 mL) was injected. The reaction mixture was stirred for 15 h at room temperature. The mixture was slowly poured into an ice-water mixture and precipitated. The solid was collected by filtration and dried under reduced pressure. Compound 3 was obtained after purification by chromatography on silica gel (eluent: cyclohexane-dichloromethane 5:5) as a yellow solid in 74% yield (0.36 g). mp 168 °C. IR (ATR) 3136, 3078, 3046, 3010, 2947, 2881, 2720, 2663, 1580, 1521, 1464, 1359, 1251, 1196, 1120, 809, 743, 690, 595, 476  $\text{cm}^{-1}$ . UV-Vis (acetonitrile)  $\lambda_{\text{max}}$  ( $\epsilon_{\text{max}}$ ,  $\text{L}\cdot\text{mol}^{-1}\cdot\text{cm}^{-1}$ ) 382 (0.42), 296 (1.13), 250 (0.88), 220 (1.60) nm.  $^1\text{H}$  NMR (400 MHz,  $\text{DMSO}-d_6$ )  $\delta$ : 9.14 (d,  $J = 1.8$  Hz, 1H), 7.69–7.62 (m, 2H), 7.62–7.55 (m, 3H), 7.46 (d,  $J = 7.4$  Hz, 2H), 7.31 (t,  $J = 7.6$  Hz, 2H), 7.27–7.19 (m, 1H), 6.83 (d,  $J = 1.8$  Hz, 1H), 4.66 (s, 2H).  $^{13}\text{C}$  NMR (100 MHz,  $\text{DMSO}-d_6$ )  $\delta$ : 148.5, 139.5, 135.2, 134.7 (2C), 130.6, 130.5 (2C), 130.3, 129.4, 129.1 (2C), 130.0 (2C), 127.8, 126.5, 126.3, 123.5, 122.7, 32.0. LC/MS ESI +  $t_{\text{R}}$  5.25 min, ( $m/z$ )  $[\text{M} + \text{H}]^+$  427.84/429.71. HRMS (+ESI): 428.0286  $[\text{M} + \text{H}]^+$ . Calcd for  $\text{C}_{20}\text{H}_{15}\text{ClN}_3\text{O}_2\text{S}_2$ : 428.0289.

**Supplementary Materials:** The following supporting information can be downloaded online. Table S1:  $^1\text{H}$  NMR,  $^{13}\text{C}$  NMR, IR and UV-Vis spectra of compound 3. Table with the in vitro data of cytotoxic and antikinoplastid references drugs. Biological Materials and Methods.

**Author Contributions:** Conceptualization, N.P.; methodology, N.P., N.A. and B.C.; validation, N.P., N.A. and B.C.; formal analysis, R.P.-L., S.B.-D., S.H. and C.B.; investigation, R.P.-L., S.B.-D., S.H., C.B. and I.J.; resources, P.V., N.A. and B.C.; writing—original draft preparation, R.P.-L.; writing—review and editing, N.P., P.V., N.A., P.R. and C.C.-D.; supervision, N.P., P.V., P.R., P.V., N.A. and B.C.; project administration, N.P. and P.V. All authors have read and agreed to the published version of the manuscript.

**Funding:** This research was funded by “Aix-Marseille Université (AMU)”, by “Centre national de la recherche scientifique (CNRS)” and by “Assistance publique-Hôpitaux de Marseille (AP-HM)”.

**Data Availability Statement:** Not applicable.

**Acknowledgments:** We want to thank Vincent Remusat (Institut de Chimie Radicalaire, Marseille) for his help with NMR analysis, Valérie Monnier and Gaëlle Hisler (Spectropole, Marseille) for performing HRMS analysis, Jean-Valère Naubron and Sara Chentouf for IR and UV-Vis spectra.

**Conflicts of Interest:** The authors declare no conflict of interest.

## References

1. Filardy, A.A.; Guimarães-Pinto, K.; Nunes, M.P.; Zukeram, K.; Fliess, L.; Pereira, L.; Nascimento, D.O.; Conde, L.; Morrot, A. Human Kinetoplastid Protozoan Infections: Where Are We Going Next? *Front. Immunol.* **2018**, *9*, 1493. [[CrossRef](#)] [[PubMed](#)]
2. Engels, D.; Zhou, X.-N. Neglected Tropical Diseases: An Effective Global Response to Local Poverty-Related Disease Priorities. *Infect. Dis. Poverty* **2020**, *9*, 10. [[CrossRef](#)] [[PubMed](#)]
3. World Health Organization (WHO). Leishmaniasis. Available online: <https://www.who.int/news-room/fact-sheets/detail/leishmaniasis> (accessed on 17 February 2023).
4. World Health Organization (WHO). Trypanosomiasis, Human African (Sleeping Sickness). 2020. Available online: [https://www.who.int/news-room/fact-sheets/detail/trypanosomiasis-human-african-\(sleeping-sickness\)](https://www.who.int/news-room/fact-sheets/detail/trypanosomiasis-human-african-(sleeping-sickness)) (accessed on 17 February 2023).
5. Burza, S.; Croft, S.L.; Boelaert, M. Leishmaniasis. *Lancet* **2018**, *392*, 951–970. [[CrossRef](#)] [[PubMed](#)]
6. Alvar, J.; Vélez, I.D.; Bern, C.; Herrero, M.; Desjeux, P.; Cano, J.; Jannin, J.; den Boer, M.; the Who Leishmaniasis Control Team. Leishmaniasis Worldwide and Global Estimates of Its Incidence. *PLoS ONE* **2012**, *7*, e35671. [[CrossRef](#)]

7. Simarro, P.P.; Cecchi, G.; Franco, J.R.; Paone, M.; Diarra, A.; Ruiz-Postigo, J.A.; Fèvre, E.M.; Mattioli, R.C.; Jannin, J.G. Estimating and Mapping the Population at Risk of Sleeping Sickness. *PLoS Neglected Trop. Dis.* **2012**, *6*, e1859. [[CrossRef](#)] [[PubMed](#)]
8. Mumba, D.; Bohorquez, E.; Messina, J.; Kande, V.; Taylor, S.M.; Tshefu, A.K.; Muwonga, J.; Kashamuka, M.M.; Emch, M.; Tidwell, R.; et al. Prevalence of Human African Trypanosomiasis in the Democratic Republic of the Congo. *PLoS Neglected Trop. Dis.* **2011**, *5*, e1246. [[CrossRef](#)] [[PubMed](#)]
9. World Health Organization (WHO). Research Priorities for Chagas Disease, Human African Trypanosomiasis and Leishmaniasis. Available online: <https://apps.who.int/iris/handle/10665/77472> (accessed on 17 February 2023).
10. Kourbeli, V.; Chontzopoulou, E.; Moschovou, K.; Pavlos, D.; Mavromoustakos, T.; Papanastasiou, I.P. An Overview on Target-Based Drug Design against Kinetoplastid Protozoan Infections: Human African Trypanosomiasis, Chagas Disease and Leishmaniasis. *Molecules* **2021**, *26*, 4629. [[CrossRef](#)] [[PubMed](#)]
11. Fersing, C.; Basmaciyan, L.; Boudot, C.; Pedron, J.; Hutter, S.; Cohen, A.; Castera-Ducros, C.; Primas, N.; Laget, M.; Casanova, M.; et al. Nongenotoxic 3-Nitroimidazo[1,2-*a*]Pyridines Are NTR1 Substrates That Display Potent *in Vitro* Antileishmanial Activity. *ACS Med. Chem. Lett.* **2019**, *10*, 34–39. [[CrossRef](#)] [[PubMed](#)]
12. Fersing, C.; Boudot, C.; Paoli-Lombardo, R.; Primas, N.; Pinault, E.; Hutter, S.; Castera-Ducros, C.; Kabri, Y.; Pedron, J.; Bourgeade-Delmas, S.; et al. Antikinetoplastid SAR Study in 3-Nitroimidazopyridine Series: Identification of a Novel Non-Genotoxic and Potent Anti-T. b. Brucei Hit-Compound with Improved Pharmacokinetic Properties. *Eur. J. Med. Chem.* **2020**, *206*, 112668. [[CrossRef](#)] [[PubMed](#)]
13. Castera, C.; Crozet, M.D.; Vanelle, P. An efficient synthetic route to new imidazo[1,2-*a*]pyridines by cross-coupling reactions in aqueous medium. *Heterocycles* **2005**, *65*, 2979–2989. [[CrossRef](#)]

**Disclaimer/Publisher’s Note:** The statements, opinions and data contained in all publications are solely those of the individual author(s) and contributor(s) and not of MDPI and/or the editor(s). MDPI and/or the editor(s) disclaim responsibility for any injury to people or property resulting from any ideas, methods, instructions or products referred to in the content.